PHYSICAL REVIEW D **93,** 065029 (2016)

Majorana neutrino mass structure induced by rigid instantons on toroidal orbifold

Tatsuo Kobayashi,[1] Yoshiyuki Tatsuta,[2] and Shohei Uemura[3]

[1]*Department of Physics, Hokkaido University, Sapporo 060-0810 Japan*
[2]*Department of Physics, Waseda University, Tokyo 169-8555, Japan*
[3]*Department of Physics, Kyoto University, Kyoto 606-8502, Japan*

(Received 10 December 2015; published 15 March 2016)

We study the effects of D-brane instantons wrapping rigid cycles on the $\mathbb{Z}_2 \times \mathbb{Z}_2'$ toroidal orbifold. We compute Majorana masses induced by rigid D-brane instantons and realize bimaximal mixing matrices in certain models. We can also derive more generic mass matrices in other models. The bimaximal mixing Majorana mass matrix provides a possibility for explaining observed mixing angles. We also compute the μ-term matrix among more than one pair of Higgs fields induced by rigid D-brane instantons.

DOI: 10.1103/PhysRevD.93.065029

I. INTRODUCTION

The Standard Model (SM) is the most successful theory in particle physics. However, a lot of mysteries still remain there. Quantum gravity theory is the biggest one, and superstring theory is the most promising (and almost only) candidate for quantum gravity theory. In addition, superstring theory may be able to unify all interactions and matters, too. Therefore, much effort has been made to understand particle physics within the framework of superstring theory. Superstring theory has no dimensionless parameters but numerous perturbative vacua. The D-brane model building is one of the interesting methods for constructing explicit vacua because one can simply realize the gauge symmetry and chiral structure of the SM [1–4] as well as other aspects. (See [5,6] for reviews.) We can construct many semirealistic models—for example, models with the SM gauge symmetry, a chiral spectrum, and the Higgs sector and no other exotics [7,8]. Our first step is to realize the SM gauge symmetry and the chiral generation spectrum. The next issue for realizing the SM would be an explanation about more detailed and quantitative aspects, e.g., the origin of hierarchy between the electroweek scale and the string scale, the flavor structure, etc.

One obstruction for D-brane models to constructing realistic models is that extra $U(1)$ symmetries of D-branes forbid some phenomenologically required terms. For instance, D-brane models often have right-handed neutrinos in order to cancel Ramond-Ramond tadpoles. From a phenomenological standpoint, heavy Majorana mass terms of right-handed neutrinos such as $\mathcal{O}(10^{10} - 10^{15})$ GeV are favored. However, extra $U(1)$ symmetries on D-branes often forbid Majorana masses of right-handed neutrinos perturbatively. In D-brane models, such perturbative symmetries can be violated by nonperturbative effects, i.e., Dp-brane instantons (or E-branes), which are Dp-branes localized at points in four-dimensional Minkowski space and are wrapping $(p+1)$-cycles on the compact space [9–13].[1]

Our purpose in this paper is to study explicitly instanton-induced Majorana masses of right-handed neutrinos as well as μ-term matrices within the framework of type IIA orientifold models, in particular, intersecting D6-brane models on toroidal orbifolds. Here, we concentrate on D2-brane instantons (or E2-branes) in IIA orientifold models compactified on the $\mathbb{Z}_2 \times \mathbb{Z}_2'$ toroidal orbifold. On the $\mathbb{Z}_2 \times \mathbb{Z}_2'$ toroidal orbifold, E2-branes can wrap rigid cycles whose position moduli in the compact space are frozen, and the positions are fixed [15]. Such a D-brane instanton can induce superpotential terms nonperturbatively, i.e., Majorana masses of right-handed neutrinos and the Higgs μ term. We will compute them explicitly and show that, for the Majorana neutrino mass matrix, there is a typical $\mathbb{Z}_2$ symmetry inherited from the geometrical symmetry of the $\mathbb{Z}_2 \times \mathbb{Z}_2'$ orbifold in certain models. For the Higgs μ-term matrix among more than one pair of Higgs fields, one D-brane instanton can make only the rank-one μ-term matrix. However, there are more than ten rigid cycles on the $\mathbb{Z}_2 \times \mathbb{Z}_2'$ orbifold, and it may be possible to make the full rank μ-term matrix.

This paper is organized as follows. In Sec. II, we review D2-brane instantons and rigid cycles on toroidal orbifolds. In Sec. III, we compute a generic form of the Majorana neutrino mass matrix induced by D-brane instantons and compute explicitly some illustrating examples. As a result, we obtain a bimaximal mixing matrix for the Majorana neutrino mass matrix in certain models. This symmetry is inherited from the geometric symmetry of the $\mathbb{Z}_2 \times \mathbb{Z}_2'$ orbifold. In Sec. IV, we also compute the Higgs μ-term matrix for more than one pair of Higgs supermultiplets. Section V is the conclusion.

[1]See also [14].

II. D-BRANE INSTANTON AND TOROIDAL ORBIFOLDS

In this section, we briefly review D-brane instanton (or E-brane) effects and rigid cycles on toroidal orbifolds. For a more detailed review of E-branes, see [6,12,13].

A. D-brane instanton

A Dp-brane instanton is a D-brane localized at a point in four-dimensional spacetime and wrapping a $(p+1)$-cycle on the six-dimensional compact space. It is similar to an instanton in gauge theory and it is called the D-brane instanton. In IIA superstring theory, there are E2-branes and we concentrate on them.

Similar to the gauge instanton, a D2-brane instanton has zero modes α_i and nonperturbative effects of the D-brane instanton are computed by integrating these zero modes,

$$\int \prod_i \mathcal{D}\alpha_i e^{-S_{\rm DBI}-S_{\rm CS}} e^{-S_{\rm interact}}, \tag{2.1}$$

where $S_{\rm DBI}$, $S_{\rm CS}$, and $S_{\rm interact}$ denote the Dirac-Born-Infeld action, the Chern-Simons term, and the interaction among zero modes of D2-brane instanton and visible matters on D6-branes, respectively. The Chern-Simons term can be written as

$$S_{\rm CS} = iN_{\rm E}\int_{\Pi_{\rm E}} C_3, \tag{2.2}$$

where $N_{\rm E}$ is the multiplicity of the E-branes. Here, $\Pi_{\rm E}$ denotes the homology class of the cycle which the E-brane wraps. We introduce $[\alpha_k]$ as the basis of 3-cycles and its dual basis $[\beta_l]$, where $[\alpha_k]\circ[\beta_l] = \delta_{kl}$. Also, we define the axion,

$$a_k = \int_{\beta_k} C_3. \tag{2.3}$$

Then, we can write

$$S_{\rm CS} = i\sum_k N_{\rm E} q_{{\rm E},k} a_k, \tag{2.4}$$

where $q_{{\rm E},k} = [\Pi_{\rm E}]\circ[\beta_k]$.

As mentioned in the previous section, the $U(1)_a$ symmetry of $U(N_a) = U(1)_a \times SU(N_a)$ on the D6$_a$-brane forbids perturbatively gauge variant operators $\mathcal{O}_c$, which transform

$$\mathcal{O}_c \to e^{iq_c\Lambda_a}\mathcal{O}_c, \tag{2.5}$$

under the $U(1)_a$ transformation $A_\mu^a \to A_\mu^a + \partial_\mu\Lambda_a$. However, the axion shifts

$$a_k \to a_k + N_a Q_{a,k}\Lambda_a, \tag{2.6}$$

under the $U(1)_a$ transformation, where $Q_{a,k} = [\alpha_k]\circ[\Pi_a]$. That leads to the following extra $U(1)_a$ transformation of instanton effects:

$$e^{-S_{\rm CS}} \to e^{-S_{\rm CS}} \exp\left(-i\sum_k N_a N_{\rm E} Q_{a,k} q_{{\rm E},k}\Lambda_a\right). \tag{2.7}$$

Thus, the E-brane effect can cancel the $U(1)$ phase in Eq. (2.5) for certain gauge variant operators, and it can generate interactions which are perturbatively forbidden by extra $U(1)$ symmetries.

The zero modes α_is are classified into two classes: neutral zero modes and charged zero modes. Neutral zero modes are not charged under gauge groups of other D-branes. Neutral zero modes are zero modes of open string stretching between a D-brane instanton. These zero modes correspond to position moduli of the D-brane instanton and their superpartners. Charged zero modes are charged under gauge groups of other D-branes. These zero modes are zero modes of open string stretching between a D-brane instanton and another D-brane. These zero modes are similar to chiral superfields.

In order to generate superpotential terms by the D-brane instanton, we need two fermionic neutral zero modes θ, which correspond to the D-brane instanton position on the superspace, and also the Goldstinos of supersymmetry broken by the D-brane instanton. Then, nonperturbative effects are expressed as

$$\int d^2\theta d^4x \prod_i \mathcal{D}\alpha_i e^{-S_{\rm DBI}-S_{\rm CS}} e^{-S_{\rm interact}}, \tag{2.8}$$

where the α_i's are charged zero modes. Finally, we can generate the nonperturbative superpotential term,

$$\mathcal{W} = \prod_i (\psi_i)^{n_i} e^{-S_{\rm DBI}}. \tag{2.9}$$

If extra neutral zero modes appear and those are not lifted up, the nonperturbatively induced superpotential term vanishes. If the E-brane can move freely in compact space, it has extra neutral zero modes. Then, we should consider the E-brane wrapping the rigid cycles.[2]

[2]In addition, to get rid of extra Goldstinos which come from $\mathcal{N}=1$ supersymmetry (SUSY) broken by an E-brane, an E-brane has to wrap a cycle which is invariant under the orientifold projection. Such a D-brane instanton is called the $O(N)$ [or $Sp(2N)$] instanton [12]. From now on, we consider rigid $O(1)$ instantons more precisely.

TABLE I. The Hodge numbers of the fractional toroidal orbifold $(T^2 \times T^2 \times T^2)/\Gamma$ having $\mathcal{N} = 1$ SUSY.

Γ	$\mathbb{Z}_3$	$\mathbb{Z}_4$	$\mathbb{Z}_6$	$\mathbb{Z}_6'$	$\mathbb{Z}_2 \times \mathbb{Z}_2$	$\mathbb{Z}_2 \times \mathbb{Z}_2'$	$\mathbb{Z}_2 \times \mathbb{Z}_4$	$\mathbb{Z}_3 \times \mathbb{Z}_3$	$\mathbb{Z}_3 \times \mathbb{Z}_6$
$h_{11}^{\rm unt}$	9	5	5	3	3	3	3	3	3
$h_{11}^{\rm twt}$	27	26	24	32	48	0	58	81	70
$h_{21}^{\rm unt}$	0	1	0	1	3	3	1	0	0
$h_{21}^{\rm twt}$	0	6	5	10	0	48	0	0	1

B. Rigid cycles on toroidal orbifolds

The toroidal orbifolds are the simple examples having rigid cycles. In Table I, we list toroidal supersymmetric orbifolds and the Hodge number of them. In this paper, we follow the notations in [15]. The orbifold twist is denoted by Γ.

For type IIA intersecting D6-brane models, nonperturbative effects originate from the D2-brane instanton wrapping the 3-cycles on compact space. The number of independent 3-cycles is given by the Betti number, $b_3 = 2 + 2h_{21}^{\rm unt} + 2h_{21}^{\rm twt}$. The bulk 3-cycles are inherited from 3-cycles on the covering torus T^6,

$$\Pi_a^B = \sum_{g\in\Gamma} \mathcal{R}_g \cdot \Pi_a^{T^6}, \tag{2.10}$$

where $\Pi_a^{T^6}$ is the ath 3-cycle on T^6 and $\mathcal{R}_g$ is the geometrical action of $g \in \Gamma$. The number of these cycles is $2 + 2h_{21}^{\rm unt}$, and these cycles have position moduli.

The number of fractional (or twisted) 3-cycles is given by $2h_{21}^{\rm twt}$. These cycles originate from orbifold fixed points and cannot move away from the fixed points. Then, they have no position moduli or zero modes.

There are five toroidal orbifolds having rigid cycles, as shown in Table I. Here, we concentrate on the $\mathbb{Z}_2 \times \mathbb{Z}_2'$ orbifold model among these five torodal orbifolds because it has the most rigid cycles, and rigid cycles on the other orbifolds have self-intersection numbers. Hence, the other rigid cycles have extra neutral zero modes. At any rate, the $\mathbb{Z}_2 \times \mathbb{Z}_2'$ orbifold is the most simple example.

C. $\mathbb{Z}_2 \times \mathbb{Z}_2'$ toroidal orbifold

Homology classes of rigid 3-cycles on the $\mathbb{Z}_2 \times \mathbb{Z}_2'$ orbifold are given by

$$\Pi_a^F = \frac{1}{4}\Pi_a^B + \frac{1}{4}\left(\sum_{i,j\in S_\Theta^a} \epsilon_{a,ij}^{\Theta}\Pi_{ij,a}^{\Theta}\right) + \frac{1}{4}\left(\sum_{j,k\in S_{\Theta'}^a} \epsilon_{a,jk}^{\Theta'}\Pi_{jk,a}^{\Theta'}\right) + \frac{1}{4}\left(\sum_{i,k\in S_{\Theta\Theta'}^a} \epsilon_{a,ik}^{\Theta\Theta'}\Pi_{ik,a}^{\Theta\Theta'}\right). \tag{2.11}$$

Here, Θ and Θ' are the generators of $\mathbb{Z}_2$ and $\mathbb{Z}_2'$, respectively. That is, Θ acts on the complex coordinates z_i on the ith T^2 as $(z_1, z_2, z_3) \to (-z_1, -z_2, z_3)$, while Θ' acts as $(z_1, z_2, z_3) \to (z_1, -z_2, -z_3)$. Also, S_g^a denotes the set of the fixed points of $\mathcal{R}_g$ which the D6$_a$-brane wraps. In addition, i, j, k are the index numbers corresponding to the fixed points on the first, second, and third T^2, respectively. i, j, k all vary from 1 to 4 and one of them represents one of four fixed points on each torus. $\epsilon_{a,ij}^g$ corresponds to the two possible orientations of the collapsed 2-cycles on the fixed point of $\mathcal{R}_g$, i.e., $\epsilon_{a,ij}^g = \pm 1$. Π_{ij}^g is the collapsed 3-cycle which can be given by

$$[\Pi_{ij}^g] = n_a^{I_g}[\alpha_{ij,n}^g] + \tilde{m}_a^{I_g}[\alpha_{ij,m}^g], \tag{2.12}$$

where $[\alpha_{ij,n}^g]$ is the product of the collapsed 2-cycle on the ith and jth fixed points of $\mathcal{R}_g$ and the 1-cycle on the other torus. The number of chiral zero modes between the Dp-branes wrapping Π_a^F and Π_b^F is given by the intersection number of rigid 3-cycles. The intersection number of rigid 3-cycles is obtained as [15]

$$\begin{aligned} I_{ab}^F &= \Pi_a^F \cdot \Pi_b^F, \\ &= \frac{1}{4} I_{ab}^{\mathbf{T}^6} + \frac{1}{4}\sum_{g\in G}\sum_{i,j\in S_g^a}\sum_{k,l\in S_g^b} \epsilon_{a,ij}^g \epsilon_{b,kl}^g \delta_{ik}\delta_{jl}(n_a^{I_g}\tilde{m}_b^{I_g} - \tilde{m}_a^{I_g} n_b^{I_g}), \\ &= \frac{1}{4} I_{ab}^{\mathbf{T}^6} + \frac{1}{4}\sum_{g\in G}\sum_{i,j\in S_g^a}\sum_{k,l\in S_g^b} \epsilon_{a,ij}^g \epsilon_{b,kl}^g \delta_{ik}\delta_{jl} I_{ab}^{I_g}. \end{aligned} \tag{2.13}$$

We need to know the physical states on the $\mathbb{Z}_2 \times \mathbb{Z}_2'$ orbifold, but not the total intersection number, in order to compute explicitly couplings of the states and the mass terms. The above number of these zero modes is interpreted as the result of a projection of zero modes on the covering space T^6. The number is equal to the number of zero modes invariant under the action of $\mathbb{Z}_2 \times \mathbb{Z}_2'$. We can write $\mathbb{Z}_2 \times \mathbb{Z}_2'$ invariant states as follows:

$$\psi_{{\rm orbifold},i} = \frac{1}{C_{\psi_i}}(\psi_i + \Delta_\Theta^\psi \psi_{\Theta i} + \Delta_{\Theta'}^\psi \psi_{\Theta' i} + \Delta_{\Theta\Theta'}^\psi \psi_{\Theta\Theta' i}), \tag{2.14}$$

where ψ_i is the state localized at the ith intersection point and C_{ψ_i} is the normalization factor of the state. For instance, if ψ_i is invariant under Θ and Θ', $C_{\psi_i} = 4$. $g \in \mathbb{Z}_2 \times \mathbb{Z}_2'$ transforms an ith intersection point to another point, $g(i)$. Δ_g^ψ is the phase of the action of $g \in \mathbb{Z}_2 \times \mathbb{Z}_2'$ determined by the sign of intersecting numbers.[3] Similar $\mathbb{Z}_N$ eigenstates are discussed in magnetized brane models [20,21]. For instance, if $\epsilon_{a,ij}^g$ and $I_{ab}^{I_g}$ are all positive, these

[3] Δ_g^ψ corresponds to the generalized Gliozzi-Scherk-Olive (GSO) phase in heterotic orbifold models. By the GSO projection, we can obtain the twist invariant states [16,17], and also the total number of massless modes, by inserting it into the partition function [18,19].

phases Δ_g^{ψ} are equal to $\Delta_g^{\psi}=1$. Then, we obtain I_{ab}^F zero modes as

$$I_{ab}^F=\frac{1}{4}I_{ab}^{\mathbf{T}^6}+\frac{1}{4}\sum_{g\in G}\sum_{i,j\in S_g^a}\sum_{k,l\in S_g^b}\delta_{ik}\delta_{jl}I_{ab}^{I_g}. \quad (2.15)$$

III. RIGHT-HANDED NEUTRINO MAJORANA MASSES

Here, we study right-handed neutrino Majorana masses on the $\mathbb{Z}_2\times\mathbb{Z}_2'$ toroidal orbifold. We concentrate on three generations of right-handed neutrinos N_R^i. They are localized at the intersection points between the D6$_a$-brane and the D6$_b$-brane wrapping the rigid cycles. The Majorana masses are perturbatively forbidden by the $U(1)$ symmetries of the D6-branes. However, they can be generated by D2-brane instanton effects. A D2-brane instanton intersects with a D6$_a$-brane and a D6$_b$-brane. Open strings at these intersection points have zero modes α_i and β_j, respectively. If there are two zero modes and they have couplings such as $d_a^{ij}\alpha_i N_R^a\beta_j$ with the three-point coupling d_a^{ij}, Majorana neutrino masses are generated as

$$M\int d^2\alpha d^2\beta e^{-d_a^{ij}\alpha_i N_R^a\beta_j}=\sum_{a,b}MN_R^aN_R^bc_{ab},$$
$$c_{ab}=\epsilon_{ij}\epsilon_{k\ell}d_a^{ik}d_b^{j\ell}, \quad (3.1)$$

where M is determined by the string scale M_s and the volume of E-branes V, like $M=M_se^{-V}$.

The three-point coupling d_{ij}^a is given by the linear combination of three-point couplings on the covering torus. Because $\mathbb{Z}_2\times\mathbb{Z}_2'$ invariant states are given by Eq. (2.14), the three-point coupling of these states is computed as

$$d_a^{ij}=\frac{1}{C_{N_R^a}C_{\alpha_i}C_{\beta_j}}\sum_{f,g,h\in\mathbb{Z}_2\times\mathbb{Z}_2'}\Delta_f^{N_R}\Delta_g^{\alpha}\Delta_h^{\beta}y_{f(a)}^{g(i)h(j)}, \quad (3.2)$$

where y_a^{ij} is the three-point coupling on the covering T^6. The three-point coupling on T^6 is obtained by a world sheet instanton. The intersection number on covering T^6 can be decomposed as $I_{ab}=I_{ab}^1I_{ab}^2I_{ab}^3$, where I_{ab}^n denotes the intersection number on the nth T^2. The three-point coupling is also decomposed as

$$y_a^{ij}=y_{a,1}^{ij}y_{a,2}^{ij}y_{a,3}^{ij}, \quad (3.3)$$

where $y_{a,n}^{ij}$ is the three-point couplings on the nth T^2. By using the ϑ function, the three-point coupling $y_{a,n}^{ij}$ is given as follows [22][4]:

$$y_{a,n}^{ij}=C\vartheta\begin{bmatrix}\frac{a}{I_{ab}^n}+\frac{i}{I_{bc}^n}+\frac{j}{I_{ca}^n}+\frac{I_{bc}^n\epsilon_a^n+I_{ca}^n\epsilon_b^n+I_{ab}^n\epsilon_c^n}{I_{ab}^nI_{bc}^nI_{ca}^n}\\ 0\end{bmatrix}$$
$$\times\left(0,\frac{iA^n|I_{ab}^nI_{bc}^nI_{ca}^n|}{4\pi^2\alpha'}\right), \quad (3.4)$$

where A^n is the area of the nth T^2, and ϵ_x^n with $x=a,b,c$ is the position moduli of the D6$_x$-brane on the nth torus. In our computations, these moduli are discretized because D-branes wrap rigid cycles. Since we consider D-branes wrapping rigid cycles, the configuration of branes on the covering T^6 is invariant under the action of $\mathbb{Z}_2\times\mathbb{Z}_2'$ and three-point couplings are also invariant, which means $y_a^{ij}=y_{g(a)}^{g(i)g(j)}$. Then, we obtain

$$d_a^{ij}=\frac{1}{C_{N_R^a}C_{\alpha_i}C_{\beta_j}}\sum_{f,g,h\in\mathbb{Z}_2\times\mathbb{Z}_2'}\Delta_f^{N_R}\Delta_g^{\alpha}\Delta_h^{\beta}y_a^{f^{-1}\cdot g(i)f^{-1}\cdot h(j)},$$
$$=\begin{cases}\frac{4}{C_{N_R^a}C_{\alpha_i}C_{\beta_j}}\sum_{g,h\in\mathbb{Z}_2\times\mathbb{Z}_2'}\Delta_g^{\alpha}\Delta_h^{\beta}y_a^{g(i)h(j)} & (\Delta_f^{N_R}\Delta_f^{\alpha}\Delta_f^{\beta}=1\quad\text{for }\forall\ f),\\ 0 & (\text{otherwise}).\end{cases} \quad (3.5)$$

As a result we can derive the Majorana masses by one instanton configuration,

$$c_{ab}=\begin{cases}\epsilon_{ij}\epsilon_{kl}\frac{16}{C_{N_R^a}C_{N_R^b}C_{\alpha_i}C_{\beta_k}C_{\alpha_j}C_{\beta_l}}\sum_{g,h,g',h'\in\mathbb{Z}_2\times\mathbb{Z}_2'}\Delta_{g\cdot g'}^{\alpha}\Delta_{h\cdot h}^{\beta}y_a^{g(i)h(k)}y_b^{g'(j)h'(l)} & (\Delta_f^{N_R}\Delta_f^{\alpha}\Delta_f^{\beta}=1\quad\text{for }\forall\ f),\\ 0 & (\text{otherwise}).\end{cases} \quad (3.6)$$

[4]Similar results for three-point couplings and higher order couplings are obtained in magnetized brane models and heterotic orbifold models [23–26].

If there is another D2-brane instanton, Majorana masses are the sum of these instantons effects, i.e.,

$$M_{ab} = \sum_m M_m \epsilon_{ij}\epsilon_{k\ell} d_a^{ik,m} d_b^{j\ell,m}. \tag{3.7}$$

We must take into account all of the possible configurations of E-branes.

The three-point couplings on covering torus (3.4) are determined by the intersection numbers on the torus. Although we assume the generation number of neutrinos to be equal to 3 and determine the number of zero modes, the intersection number on the covering torus is not uniquely determined because the intersection number on orbifold (2.13) depends on the choice of fixed points. It is difficult to consider all of the possibilities, although we would study them systematically elsewhere. In this paper, we compute some explicit examples to conjecture about the general form of the Majorana masses.

In toroidal orientifolds, there are two types of T^2: the rectangular torus whose complex structure $\mathrm{Re}\tau = 0$ and the tilted torus with $\mathrm{Re}\tau = 1/2$. In our analysis, we concentrate on the rectangular torus for simplicity, but this limitation dose not affect our results.

We use the notation $(l, m, n)_{xy}$ as the abbreviation for the number of fixed points shared by the D6$_x$-brane and the D6$_y$-brane, where l represents the number of fixed points shared by the D6$_x$-brane and the D6$_y$-brane on the first T^2, and m and n are those on the second and third T^2's. For example, $(l, m, n)_{xx}$ is always $(2, 2, 2)_{xx}$.

A. Explicit model 1

In this section, we compute Majorana neutrino masses in an explicit example.[5] We consider only D6-branes relating to the right-handed neutrinos and the E-brane, but we do not study complete model building. We compute the model with $(1, 0, 0)_{ab}, (1, 1, 1)_{Ea}$, and $(1, 1, 1)_{Eb}$ because this is the simplest model with three generations of neutrinos. In this model, the intersection number is

$$I^F_{ab} = \frac{1}{4} I^1_{ab} I^2_{ab} I^3_{ab}. \tag{3.8}$$

There are only two independent solutions in this model,

$$\begin{cases} I^1_{ab} = 1, & I^2_{ab} = 6, & I^3_{ab} = 2. & \text{(I)} \\ I^1_{ab} = 3, & I^2_{ab} = 2, & I^3_{ab} = 2, & \text{(II)} \end{cases} \tag{3.9}$$

[5]In the following examples, we consider only the intersection numbers. To construct more concrete models, we should set the winding numbers and ensure the stability of branes, too. In principle, there may be no solutions for realizing the desired intersection in some cases. However, we have three complex structures as free parameters. It is often possible to tune them to stabilize the branes. In Appendix B, we show it in model 1-(I).

In these models, there are 12 (would-be neutrino) states on the covering torus. We name these (would-be neutrino) states $|ijk\rangle_\nu$, where i, j, and k represent the index number of fixed points on the first, second, and third torus, respectively.

For model 1-(I), we have $i = 0. j = 0, \cdots 5$ and $k = 0, 1$. These states transform under $\mathbb{Z}_2$ and $\mathbb{Z}_2'$ as

$$\begin{aligned} &\mathbb{Z}_2 : |0jk\rangle_\nu \to |0(5-j)k\rangle_\nu, \\ &\mathbb{Z}_2' : |0jk\rangle_\nu \to |0(5-j)(1-k)\rangle_\nu. \end{aligned} \tag{3.10}$$

Then, we can write three invariant neutrino states,

$$\begin{aligned} N_0 &= \frac{1}{\sqrt{4}}(|000\rangle_\nu + |050\rangle_\nu + |051\rangle_\nu + |001\rangle_\nu), \\ N_1 &= \frac{1}{\sqrt{4}}(|010\rangle_\nu + |040\rangle_\nu + |041\rangle_\nu + |011\rangle_\nu), \\ N_2 &= \frac{1}{\sqrt{4}}(|020\rangle_\nu + |030\rangle_\nu + |031\rangle_\nu + |021\rangle_\nu). \end{aligned} \tag{3.11}$$

For model 1-(II), we can write three invariant neutrino states similarly:

$$\begin{aligned} N_0 &= \frac{1}{\sqrt{4}}(|000\rangle_\nu + |010\rangle_\nu + |011\rangle_\nu + |001\rangle_\nu), \\ N_1 &= \frac{1}{\sqrt{4}}(|100\rangle_\nu + |210\rangle_\nu + |111\rangle_\nu + |201\rangle_\nu), \\ N_2 &= \frac{1}{\sqrt{4}}(|200\rangle_\nu + |110\rangle_\nu + |211\rangle_\nu + |101\rangle_\nu). \end{aligned} \tag{3.12}$$

The intersection number between the D2-brane instanton and the D6$_a$-brane must satisfy the following condition:

$$I^F_{Ea} = \frac{1}{4} I^1_{Ea} I^2_{Ea} I^3_{Ea} + \frac{1}{4} I^3_{Ea} + \frac{1}{4} I^1_{Ea} + \frac{1}{4} I^2_{Ea} = 2. \tag{3.13}$$

There is only one independent solution, $(I^1_{Ea}, I^2_{Ea}, I^3_{Ea}) = (\underline{3, 1, 1})$, where the underline denotes all of the possible permutations. The physically invariant zero-mode states α_i can be written as

$$\begin{aligned} \alpha_0 &= |000\rangle_\alpha, \\ \alpha_1 &= \frac{1}{\sqrt{2}}(|100\rangle_\alpha + |200\rangle_\alpha), \end{aligned} \tag{3.14}$$

for the model with $(I^1_{Ea}, I^2_{Ea}, I^3_{Ea}) = (3, 1, 1)$ by using (would-be zero-mode) states $|ijk\rangle_\alpha$. Similarly, we can write the invariant states β_i, i.e.,

$$\beta_0 = |000\rangle_\beta,$$
$$\beta_1 = \frac{1}{\sqrt{2}}(|100\rangle_\beta + |200\rangle_\beta). \tag{3.15}$$

When the three generations of neutrinos (3.11) or (3.12) and instanton zero modes (3.14) appear from different tori, induced Majorana masses vanish [14]. Therefore, there are only two solutions leading to nonvanishing Majorana masses. One is the model with $(I^1_{ab}, I^2_{ab}, I^3_{ab}) = (1, 6, 2)$ and $(I^1_{Ea}, I^2_{Ea}, I^3_{Ea}) = (I^1_{Eb}, I^2_{Eb}, I^3_{Eb}) = (1, 3, 1)$. The other is $(I^1_{ab}, I^2_{ab}, I^3_{ab}) = (3, 2, 2)$ and $(I^1_{Ea}, I^2_{Ea}, I^3_{Ea}) = (I^1_{Eb}, I^2_{Eb}, I^3_{Eb}) = (3, 1, 1)$. Other solutions have vanishing Majorana masses because they are canceled by the completely antisymmetric tensor ϵ_{ab}.

The interaction term of model 1-(I) is written as follows[6]:

$$\begin{aligned} S_{\text{interact}} = {} & \sqrt{2}y^1 y^2_2 y^3 \alpha_0\beta_1 N_0 + \sqrt{2}y^1 y^2_0 y^3 \alpha_1\beta_0 N_0 \\ & + y^1 y^2_1 y^3 \alpha_1\beta_1 N_0 + \sqrt{2}y^1 y^2_0 y^3 \alpha_0\beta_1 N_2 \\ & + \sqrt{2}y^1 y^2_2 y^3 \alpha_1\beta_0 N_2 + y^1 y^2_1 y^3 \alpha_1\beta_1 N_2 \\ & + 2y^1 y^2_1 y^3 \alpha_0\beta_0 N_1 + y^1(y^2_0 + y^2_2) y^3 \alpha_1\beta_1 N_1, \end{aligned} \tag{3.16}$$

where y^j_i is the three-point coupling on the jth torus written as (3.4). These interactions are determined by $\mathbb{Z}_3$ symmetries of the second torus. We can derive the following Majorana masses:

$$\begin{aligned} M_{R,ij} \propto {} & (y^1 y^3)^2 \\ & \times \begin{pmatrix} 2y^2_0 y^2_2 & -(y^2_1)^2 & (y^2_0)^2 + (y^2_2)^2 \\ -(y^2_1)^2 & -2y^2_1(y^2_0 + y^2_2) & -(y^2_1)^2 \\ (y^2_0)^2 + (y^2_2)^2 & -(y^2_1)^2 & 2y^2_0 y^2_2 \end{pmatrix} \end{aligned} \tag{3.17}$$

$$= \begin{pmatrix} A & B & C \\ B & D & B \\ C & B & A \end{pmatrix}. \tag{3.18}$$

Similarly, the Majorana masses of model 1-(II) are computed as

$$\begin{aligned} M_{R,ij} \propto {} & (y^2 y^3)^2 \begin{pmatrix} y^1_0 y^1_1 & -\frac{1}{4}(y^1_0)^2 & -\frac{1}{4}(y^1_0)^2 \\ -\frac{1}{4}(y^1_0)^2 & \frac{1}{2}(y^1_1)^2 & \frac{1}{2}(y^1_1)^2 \\ -\frac{1}{4}(y^1_0)^2 & \frac{1}{2}(y^1_1)^2 & \frac{1}{2}(y^1_1)^2 \end{pmatrix} \\ = {} & \begin{pmatrix} A & B & B \\ B & C & C \\ B & C & C \end{pmatrix}. \end{aligned} \tag{3.19}$$

[6]For more details, see Appendix A.

In these models, apparent $\mathbb{Z}_2$ symmetric (or bimaximal mixing) Majorana mass matrices appear.

B. Explicit model 2

We now study another model. We consider the model with $(1, 1, 0)_{ab}, (1, 1, 1)_{Ea}$, and $(0, 1, 1)_{Eb}$. In this model, since the E-a intersection number and the shared fixed points are the same as the last model, the physical state α_i's are the same as in Eq. (3.14). The a–b intersection and E–b intersection conditions have a solution

$$\begin{aligned} & I^1_{ab} = 5, \quad I^2_{ab} = 1, \quad I^3_{ab} = 2, \\ & I^1_{Eb} = 4, \quad I^2_{Eb} = I^3_{Eb} = 1, \end{aligned} \tag{3.20}$$

and the physical states of neutrinos are written as

$$\begin{aligned} N_0 &= \frac{1}{\sqrt{2}}(|000\rangle_\nu + |001\rangle_\nu), \\ N_1 &= \frac{1}{\sqrt{4}}(|100\rangle_\nu + |400\rangle_\nu + |101\rangle_\nu + |401\rangle_\nu), \\ N_2 &= \frac{1}{\sqrt{4}}(|200\rangle_\nu + |300\rangle_\nu + |201\rangle_\nu + |301\rangle_\nu). \end{aligned} \tag{3.21}$$

The zero mode β_i's are

$$\begin{aligned} \beta_0 &= \frac{1}{\sqrt{2}}(|000\rangle_\beta + |300\rangle_\beta), \\ \beta_1 &= \frac{1}{\sqrt{2}}(|100\rangle_\beta + |200\rangle_\beta). \end{aligned} \tag{3.22}$$

Then, we can obtain nonvanishing Majorana masses. In this model, the Majorana mass matrix has no apparent symmetry without fine-tunings but corresponds to general symmetric Majorana masses with the full rank.

C. Flavor structure of the Majorana mass matrix

We computed Majorana masses in explicit models [27]. In model 1, we derived the bimaximal mixing mass matrix, and the other model does not have such a symmetry. This difference originates from the geometric symmetry of D-brane configurations on the torus.

There are two geometric symmetries in models 1-(I) and 1-(II). In model 1-(I), the flavor structure originates from the second torus. On the second torus, there is $\mathbb{Z}_2$ symmetry acting on the branes by exchanging the a-brane and the b-brane and exchanging two fixed points simultaneously. This symmetry exchanges N_0, α_i and N_2, β_i but does not change the areas of world sheet instantons. Then, the three-point couplings are the same (see Fig. 1). In model 1-(II), the flavor structure originates from the first torus. However, there are no differences between N_1 and N_2 and the system is invariant under exchanging N_1 and N_2. Thus, we realize the $\mathbb{Z}_2$ permutation symmetry and bimaximal mixing mass matrix.

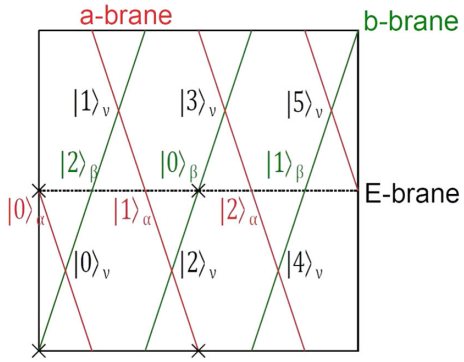

FIG. 1. The brane configuration on the second torus of model 1-(I). We omit the index number of other tori; e.g., $|0\rangle_\alpha$ denotes $|000\rangle_\alpha$. The others are similar.

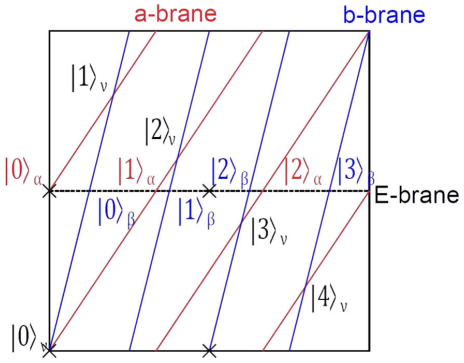

FIG. 2. The brane configuration on the first torus of model 2. We omit the index number of other tori; e.g., $|0\rangle_\alpha$ denotes $|000\rangle_\alpha$ The others are similar.

On the other hand, in model 2, such $\mathbb{Z}_2$ symmetries no longer remain. The flavor structure originates from the second torus. We cannot exchange N_1 and N_2 or fixed points (see Fig. 2). The only symmetry is $\mathbb{Z}_2$: $z \to -z$, which is orbifold projection. We can distinguish each state from the others. Thus, we get general symmetric mass matrix.

It is phenomenologically interesting that the $\mathbb{Z}_2$ symmetry remains in Majorana masses of right-handed neutrinos. Such a symmetry would be favorable for deriving a large mixing angle in the lepton sector. Indeed, many studies have been done for realization of the observed lepton mixing angles by assuming non-Abelian discrete flavor symmetries. (See [28–30] for reviews.)[7]

D. Numerical analysis

In this subsection, we analyze the lepton flavor structure numerically for illustration. To compute the mixing angles of leptons and mass splittings, we have to determine the Dirac mass matrix of leptons, the number of Higgs fields and vacuum expectation values (VEVs) of Higgs fields. In our analysis, left-handed lepton L_i's are localized at the intersection points of the D6$_a$-brane and the D6$_c$-brane. The up-type Higgs field H_u's are localized at the intersection points of the D6$_b$-brane and the D6$_c$-brane. All of the branes are wrapping rigid cycles. Indeed, there are many possibilities for the charged lepton sector.[8] Results depend on its choice. To illustrate the numerical study, we assume that the Dirac masses of the charged leptons are diagonal and that they are equal to the observed charged lepton masses, and the mixing angles of leptons are determined by the Dirac and Majorana masses of neutrinos. They are determined by the area of the torus, and the VEVs of the Higgs fields. We do not compute the Higgs potential in this analysis, and we use their VEVs as free parameters.

In Table II, we show two examples of mixing angles and neutrino mass splittings given by D-brane instanton effects. In these examples, there are two Higgs doublets in the models. Then, there are three parameters: the area of torus A_1/α', the ratio of Higgs VEVs $\langle H_{u1}\rangle/\langle H_{u0}\rangle$, and the scale of Majorana masses $M_s e^{-S_E}$.[9]

In example 1, the Majorana mass matrix is the same as in model 1-(I) in the previous subsection (3.18). We set the winding numbers as

$$I^1_{ac} = 1, \quad I^2_{ac} = 5, \quad I^3_{ac} = 1,$$
$$I^1_{bc} = 1, \quad I^2_{bc} = 2, \quad I^3_{bc} = 1. \tag{3.23}$$

The numbers of shared fixed points are $(1,1,1)_{ac}$ and $(1,2,1)_{bc}$. In example 1, we set the area of torus $A_2/\alpha' = 0.6$ and the Higgs VEV ratio $\langle H_{u1}\rangle/\langle H_{u0}\rangle = 0.2$.

In example 2, the Majorana mass matrix is the same as the explicit model 2 in the previous subsection. We set the winding numbers as

$$I^1_{ac} = 4, \quad I^2_{ac} = 1, \quad I^3_{ac} = 1,$$
$$I^1_{bc} = 2, \quad I^2_{bc} = 1, \quad I^3_{bc} = 1. \tag{3.24}$$

The numbers of shared fixed points are $(2,1,1)_{ac}$ and $(1,2,1)_{bc}$. In example 2, we set the area of torus $A_1/\alpha' = 2.3$ and the Higgs VEV ratio $\langle H_{u1}\rangle/\langle H_{u0}\rangle = 0.3$.

Table II shows that we can realize the approximate values of the mixing angles and the mass splitting of neutrinos by E-branes, but there are the small deviations between theoretical and observed values. These deviations may

[7]Moreover, it is found that non-Abelian discrete flavor symmetries appear at perturbative level in heterotic orbifold models [17,31] and intersecting/magnetized brane models [32,33].

[8]For three-generation models on magnetized orbifold models, see, e.g., [26,34], and those would correspond to T-duals of intersecting D-brane models.

[9]More precisely, there is one more parameter, the overall scales of Higgs VEVs. However, we can absorb it in the scale of Majorana masses and it does not affect our analysis.

TABLE II. Sample values of a numerical analysis of the lepton flavor structure. The observed values are quoted from [35,36]. In our analysis, we assume the normal hierarchy.

Observables	Example 1	Example 2	Observed values
$(m_{\nu_1}, m_{\nu_2}, m_{\nu_3})$ [eV]	(0.017,0.018,0.052)	(0.000026,0.00011,0.051)	< 2.0
$\lvert m_{\nu_2}^2 - m_{\nu_1}^2 \rvert$ [eV^2]	4.8×10^{-5}	1.2×10^{-8}	7.62×10^{-5}
$\lvert m_{\nu_3}^2 - m_{\nu_2}^2 \rvert$ [eV^2]	2.4×10^{-3}	2.6×10^{-3}	2.55×10^{-3}
$\sin^2\theta_{12}$	0.341	0.253	0.259–0.359
$\sin^2\theta_{23}$	0.758	0.827	0.380–0.628
$\sin^2\theta_{13}$	0.0212	0.0603	0.0176–0.0295

be caused by the assumptions of the diagonal charged lepton mass matrix. Small deviations from the diagonal charged lepton mass matrix could explain the observed data. At any rate, our purpose in this subsection is just an illustration of numerical study.

IV. HIGGS μ-TERM MATRIX

We can also obtain Higgs μ terms by E2-branes. We consider g pairs of Higgs fields H_u and H_d. We assume that the H_u's are localized at the intersection points of the D6$_a$-brane and the D6$_b$-brane, and the H_d's are localized at the intersection points of the D6$_a$-brane and the D6$_c$-brane. The multiplicity of the D6$_a$-brane is 2, and the others are 1. To generate μ terms, the E-brane intersects other branes once, and there are three kinds of zero modes: α, β, γ. α is localized at the E-a intersection point, β is localized at the E-b intersection point, and γ is at the E-c intersection point. Then, we obtain the μ term,

$$\int \mathcal{D}^2\alpha\mathcal{D}\gamma\mathcal{D}\beta M_s e^{-S_E} e^{y_i^u \alpha\cdot H_u^i \beta + y_j^d \alpha\cdot H_d^j \gamma} = M_s e^{-S_E} y_i^u y_j^d H_u^i \cdot H_d^j. \quad (4.1)$$

This matrix shows that one instanton configuration can generate only a rank-one μ-term matrix. Let us consider the model with two-pair Higgs fields, for instance. We study the model with $(1,1,1)_{ab,c}$, $(0,0,0)_{bc}$, $(1,1,1)_{Ea,b,c}$. In this model, the intersection number can have the following solution:

$$I_{ab}^1 = I_{ac}^1 = 3, \quad I_{ab}^2 = I_{ac}^2 = 1, \quad I_{ab}^3 = I_{ac}^3 = 1,$$
$$I_{bc}^i = 0 \quad (\text{for } \forall\ i \in \{1,2,3\}),$$
$$I_{Ex}^1 = I_{Ex}^2 = I_{Ex}^3 = 1 \quad (\text{for } \forall\ x \in \{a,b,c\}). \quad (4.2)$$

Then, we obtain the rank-one μ-term matrix similarly:

$$\mu_{ij} \propto \begin{pmatrix} y_0^u y_0^d & y_0^u y_1^d \\ y_1^u y_0^d & y_1^u y_1^d \end{pmatrix}, \quad (4.3)$$

where $y_i^{u(d)}$ is the three-point coupling of the ith Higgs field $H_{u(d)}^i$ and zero modes on the first torus. Because those on the other torus are common, we omit the indices of the torus. If there is nothing to obstruct, we also take into account the contribution of the E-brane (the E$\prime$-brane in Fig. 3) wrapping the other fixed points on the first torus and having the same winding number. Thus, we get the rank-two symmetric μ-term matrix

$$\mu_{ij} \propto \begin{pmatrix} 2y_0^u y_0^d & y_0^u y_1^d + y_1^u y_0^d \\ y_0^u y_1^d + y_1^u y_0^d & 2y_1^u y_1^d \end{pmatrix}. \quad (4.4)$$

This expression is inherited from the symmetry of the configurations of D-branes, too. The configuration is invariant under exchanging the fixed points and b,c-branes simultaneously. Then, such an expression appears. The rank of the μ-term matrix depends on the number of allowed configurations of E-branes. In this example, there are two configurations and we get a rank-two matrix. If the number of Higgs pairs is larger than two, we cannot realize the full rank μ term by one type of E-branes. However, there are some possibilities that the configuration of rigid E-branes wrapping another bulk cycle can also induce some corrections for μ terms. The suppression factor of the E-brane is $e^{-S_{\rm DBI}}$. Although the leading order E-brane induces high-scale μ terms, e.g., $\mathcal{O}(10^{10-15})$ GeV, the next to leading order term may be more suppressed. In addition to that, the μ terms induced by E-branes is a product of the

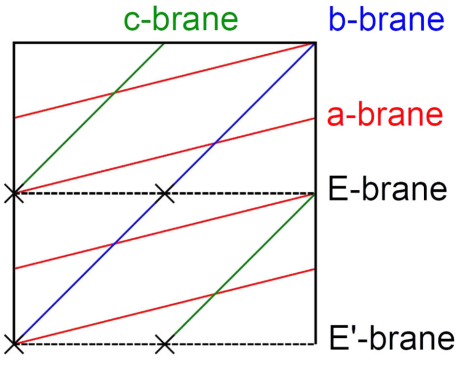

FIG. 3. The brane configuration on the first torus. The intersection numbers of the E$\prime$-brane and other branes are the same as those of the E-brane and other branes.

three-point couplings. The three-point couplings are suppressed by the world sheet area. If the compactification scale is large enough, the Yukawa couplings are suppressed. We may realize the low scale μ term naturally like this and solve the "μ-problem."

V. CONCLUSION AND DISCUSSION

We have studied the effects of E-branes on the $\mathbb{Z}_2 \times \mathbb{Z}_2'$ toroidal orbifold. On this orbifold, there are rigid cycles which cannot move away from the fixed points and have no position moduli. The D-brane instanton wrapping such cycles can induce a nonperturbative superpotential.

In this paper, we have concentrated on the Majorana masses of right-handed neutrinos as well as Higgs μ terms. We have computed the general form of Majorana neutrino masses and computed them explicitly in concrete models. As a result, we have realized the bimaximal mixing Majorana mass matrix, although we have also been able to obtain a not so symmetric one. This symmetry originates from geometric configurations of branes. From a phenomenological point of view, such a Majorana mass matrix is interesting because one could derive the observed large mixing angles by using such a symmetry. In fact, we find some examples roughly fitting the mixing angles and the neutrino mass splittings.

We also computed the Higgs μ-term matrix in an explicit model and have obtained rank-one and rank-two μ-term matrices. This is because one D-brane instanton can only make a rank-one matrix and the rigid E-brane wrapping the same bulk cycle has, at most, two configurations. However, we can consider another E-brane configuration and may derive the full rank μ-term matrix. Such a configuration may induce a suppressed term and may explain the electroweak scale. We will study this elsewhere.

It is important to study other compactifications. If D-brane configurations including D-brane instantons have geometrical symmetries such as $\mathbb{Z}_2$ symmetry, Majorana neutrino masses would respect such symmetries and would lead to phenomenologically interesting results even in more complicated compactifications.

ACKNOWLEDGMENTS

T. K. and S. U. are supported in part by Grants-in-Aid for Scientific Research No. 25400252 and No. 15J02107 from the Ministry of Education, Culture, Sports, Science and Technology in Japan.

APPENDIX A: YUKAWA COUPLINGS OF ZERO MODES AND NEUTRINOS

In this appendix, we compute the Yukawa couplings of zero modes and neutrinos explicitly in a model. We study model 1-(I) in Sec. III A. In this model, there are two branes (the a-brane and the b-brane) and one E-brane. Their intersection numbers are

$$(I^1_{ab}, I^2_{ab}, I^3_{ab}) = (1, 6, 2),$$
$$(I^1_{Ea}, I^2_{Ea}, I^3_{Ea}) = (I^1_{Eb}, I^2_{Eb}, I^3_{Eb}) = (1, 3, 1). \quad \text{(A1)}$$

The flavor structure of neutrinos and zero modes originates from the second torus, and we concentrate on that. The brane configuration on the second torus is shown in Fig. 1.

Before computing Yukawa couplings, it is worth considering the geometrical symmetry of this configuration. For example, since the area of the triangle whose vertices are $|0\rangle_\nu$, $|0\rangle_\alpha$, and $|2\rangle_\beta$ is the same as that of the triangle surrounded by $|1\rangle_\nu$, $|1\rangle_\alpha$, and $|2\rangle_\beta$, y_{002} is equal to y_{112}. Similarly, we obtain three equations:

$$y_{001} = y_{112} = y_{210} = y_{320} = y_{421} = y_{501} = y_0,$$
$$y_{011} = y_{100} = y_{222} = y_{311} = y_{400} = y_{522} = y_1,$$
$$y_{020} = y_{121} = y_{201} = y_{302} = y_{412} = y_{510} = y_2, \quad \text{(A2)}$$

and other couplings are forbidden. Each coupling is written by a theta function:

$$y_0 = C\vartheta\begin{bmatrix}\frac{1}{12}\\ 0\end{bmatrix}\left(0, \frac{i6\pi A}{\alpha'}\right), \quad \text{(A3)}$$

$$y_1 = C\vartheta\begin{bmatrix}\frac{3}{12}\\ 0\end{bmatrix}\left(0, \frac{i6\pi A}{\alpha'}\right), \quad \text{(A4)}$$

$$y_2 = C\vartheta\begin{bmatrix}\frac{5}{12}\\ 0\end{bmatrix}\left(0, \frac{i6\pi A}{\alpha'}\right), \quad \text{(A5)}$$

where C is the common factor of quantum corrections and A is the area of the second torus. The Yukawa couplings of the invariant states are the linear combinations of them. We can express these couplings as

$$d^{00}_0 = 0, \quad d^{01}_0 = \sqrt{2}y_2, \quad d^{10}_0 = \sqrt{2}y_0, \quad d^{11}_0 = y_1,$$
$$d^{00}_1 = 2y_1, \quad d^{01}_1 = 0, \quad d^{10}_1 = 0, \quad d^{11}_1 = y_0 + y_2,$$
$$d^{00}_2 = 0, \quad d^{01}_2 = \sqrt{2}y_0, \quad d^{10}_2 = \sqrt{2}y_2, \quad d^{11}_2 = y_1, \quad \text{(A6)}$$

where d^{ij}_a denotes the Yukawa coupling of the neutrino N_a and the zero modes α_i, β_j.

Finally, we obtain the interaction terms of Eq. (3.16) and the Majorana mass matrix of Eq. (3.18).

APPENDIX B: WINDING NUMBERS OF MODEL 1-(I)

In this appendix, we show one solution of the winding numbers of model 1-(I) in Sec. III A and provide some more details. We study the rectangular torus model in this appendix. One solution of the winding numbers is

$$(n_a^1, m_a^1) = (1,1), \quad (n_a^2, m_a^2) = (1,-3), \quad (n_a^3, m_a^3) = (1,1),$$
$$(n_b^1, m_b^1) = (1,2), \quad (n_b^2, m_b^2) = (1,3), \quad (n_b^3, m_b^3) = (1,3),$$
$$(n_E^1, m_E^1) = (0,1), \quad (n_E^2, m_E^2) = (1,0), \quad (n_E^3, m_E^3) = (0,1), \tag{B1}$$

where n_a^i denotes the winding number of the x axis on ith torus and m_x^i denotes the winding number of the y axis on the ith torus. In this model, the open string spectrum stretching between the a-brane and the b-brane is determined as

$$m^2 = \theta_{ab}^1 \pm \theta_{ab}^2 \pm \theta_{ab}^3, \tag{B2}$$

where θ_{ab}^i is the angle between the a-brane and the b-brane on the ith torus. If one of the equations (B2) is equal to zero, a part of SUSY is conserved and the configuration is stable. In fact, we can find solutions of them. For example, if $\tau_1 = 4.05$, $\tau_2 = 0.1$, and $\tau_3 = 1$, $\theta_{ab}^1 - \theta_{ab}^2 + \theta_{ab}^3 \simeq 0$. As the limit of τ infinity (or zero), the angle between a brane and a horizontal axis approaches 0 or $\pi/2$. Then, one of the equations (B2) could be zero unless some winding numbers are 0.

In this model, there are two other E-branes having the desired zero-mode structures. One is

$$(n_{E'}^1, m_{E'}^1) = (0,-1), \quad (n_{E'}^2, m_{E'}^2) = (-1,0),$$
$$(n_{E'}^3, m_{E'}^3) = (1,0), \tag{B3}$$

and the other is

$$(n_{E''}^1, m_{E''}^1) = (1,0), \quad (n_{E''}^2, m_{E''}^2) = (-1,0),$$
$$(n_{E''}^3, m_{E''}^3) = (0,-1). \tag{B4}$$

The fixed points are $(1,1,1)_{E'a}$, $(1,1,1)_{E'b}$ and $(1,1,1)_{E''a}$, $(2,1,1)_{E''b}$. Though these E-branes have the desired zero-mode structures, their effect is canceled out by the sign condition of Eq. (3.6) and cannot induce Majorana masses. The Majorana mass matrix (3.18) is not affected by other E-branes.

[1] M. Berkooz, M. R. Douglas, and R. G. Leigh, Branes intersecting at angles, Nucl. Phys. **B480**, 265 (1996).

[2] R. Blumenhagen, L. Goerlich, B. Kors, and D. Lust, Noncommutative compactifications of type I strings on tori with magnetic background flux, J. High Energy Phys. 10 (2000) 006.

[3] G. Aldazabal, S. Franco, L. E. Ibanez, R. Rabadan, and A. M. Uranga, $D = 4$ chiral string compactifications from intersecting branes, J. Math. Phys. (N.Y.) **42**, 3103 (2001); J. High Energy Phys. 02 (2001) 047.

[4] C. Angelantonj, I. Antoniadis, E. Dudas, and A. Sagnotti, Type I strings on magnetized orbifolds and brane transmutation, Phys. Lett. B **489**, 223 (2000).

[5] R. Blumenhagen, B. Kors, D. Lust, and S. Stieberger, Four-dimensional string compactifications with D-branes, orientifolds and fluxes, Phys. Rep. **445**, 1 (2007).

[6] L. E. Ibanez and A. M. Uranga, *String Theory and Particle Physics: An Introduction to String Phenomenology* (Cambridge University Press, Cambridge, England, 2012).

[7] M. Cvetic, G. Shiu, and A. M. Uranga, Chiral four-dimensional $N = 1$ supersymmetric type 2A orientifolds from intersecting D6 branes, Nucl. Phys. **B615**, 3 (2001).

[8] L. E. Ibánez, F. Marchesano, and R. Rabadan, Getting just the standard model at intersecting branes, J. High Energy Phys. 11 (2001) 002.

[9] R. Blumenhagen, M. Cvetic, and T. Weigand, Spacetime instanton corrections in 4D string vacua: The seesaw mechanism for D-brane models, Nucl. Phys. **B771**, 113 (2007).

[10] R. Blumenhagen, M. Cvetic, S. Kachru, and T. Weigand, D-brane instantons in type II orientifolds, Annu. Rev. Nucl. Part. Sci. **59**, 269 (2009).

[11] L. E. Ibanez and A. M. Uranga, Neutrino Majorana masses from string theory instanton effects, J. High Energy Phys. 03 (2007) 052.

[12] L. E. Ibanez, A. N. Schellekens, and A. M. Uranga, Instanton induced neutrino Majorana masses in CFT orientifolds with MSSM-like spectra, J. High Energy Phys. 06 (2007) 011; S. Antusch, L. E. Ibanez, and T. Macri, Neutrino masses and mixings from string theory instantons, J. High Energy Phys. 09 (2007) 087.

[13] M. Cvetic, R. Richter, and T. Weigand, Computation of D-brane instanton induced superpotential couplings: Majorana masses from string theory, Phys. Rev. D **76**, 086002 (2007).

[14] Y. Hamada, T. Kobayashi, and S. Uemura, Flavor structure in D-brane models: Majorana neutrino masses, J. High Energy Phys. 05 (2014) 116; H. Abe, T. Kobayashi, Y. Tatsuta, and S. Uemura, D-brane instanton induced μ terms and their hierarchical structure, Phys. Rev. D **92**, 026001 (2015).

[15] R. Blumenhagen, M. Cvetic, F. Marchesano, and G. Shiu, Chiral D-brane models with frozen open string moduli, J. High Energy Phys. 03 (2005) 050.

[16] T. Kobayashi and N. Ohtsubo, Yukawa coupling condition of $Z(N)$ orbifold models, Phys. Lett. B **245**, 441 (1990); Geometrical aspects of Z_N orbifold phenomenology, Int. J. Mod. Phys. A **09**, 87 (1994).

[17] T. Kobayashi, S. Raby, and R. J. Zhang, Searching for realistic 4d string models with a Pati-Salam symmetry: Orbifold grand unified theories from heterotic string

compactification on a Z_6 orbifold, Nucl. Phys. **B704**, 3 (2005).

[18] L. E. Ibanez, J. Mas, H. P. Nilles, and F. Quevedo, Heterotic strings in symmetric and asymmetric orbifold backgrounds, Nucl. Phys. **B301**, 157 (1988).

[19] I. Senda and A. Sugamoto, Orbifold models and modular transformation, Nucl. Phys. **B302**, 291 (1988).

[20] H. Abe, T. Kobayashi, and H. Ohki, Magnetized orbifold models, J. High Energy Phys. 09 (2008) 043.

[21] T. H. Abe, Y. Fujimoto, T. Kobayashi, T. Miura, K. Nishiwaki, and M. Sakamoto, Z_N twisted orbifold models with magnetic flux, J. High Energy Phys. 01 (2014) 065; Operator analysis of physical states on magnetized T^2/Z_N orbifolds, Nucl. Phys. **B890**, 442 (2014).

[22] M. Cvetic and I. Papadimitriou, Conformal field theory couplings for intersecting D-branes on orientifolds, Phys. Rev. D **68**, 046001 (2003); **70**, 029903(E) (2004); S. A. Abel and A. W. Owen, Interactions in intersecting brane models, Nucl. Phys. **B663**, 197 (2003); D. Cremades, L. E. Ibanez, and F. Marchesano, Yukawa couplings in intersecting D-brane models, J. High Energy Phys. 07 (2003) 038; S. A. Abel and A. W. Owen, N-point amplitudes in intersecting brane models, Nucl. Phys. **B682**, 183 (2004).

[23] D. Cremades, L. E. Ibanez, and F. Marchesano, Computing Yukawa couplings from magnetized extra dimensions, J. High Energy Phys. 05 (2004) 079.

[24] H. Abe, K. S. Choi, T. Kobayashi, and H. Ohki, Higher order couplings in magnetized brane models, J. High Energy Phys. 06 (2009) 080.

[25] S. Hamidi and C. Vafa, Interactions on orbifolds, Nucl. Phys. **B279**, 465 (1987); L. J. Dixon, D. Friedan, E. J. Martinec, and S. H. Shenker, The conformal field theory of orbifolds, Nucl. Phys. **B282**, 13 (1987); T. T. Burwick, R. K. Kaiser, and H. F. Muller, General Yukawa couplings of strings on Z_N orbifolds, Nucl. Phys. **B355**, 689 (1991); J. Erler, D. Jungnickel, M. Spalinski, and S. Stieberger, Higher twisted sector couplings of Z(N) orbifolds, Nucl. Phys. **B397**, 379 (1993); K.-S. Choi and T. Kobayashi, Higher order couplings from heterotic orbifold theory, Nucl. Phys. **B797**, 295 (2008).

[26] T. H. Abe, Y. Fujimoto, T. Kobayashi, T. Miura, K. Nishiwaki, M. Sakamoto, and Y. Tatsuta, Classification of three-generation models on magnetized orbifolds, Nucl. Phys. **B894**, 374 (2015).

[27] We study Majorana masses induced by only one D-brane instanton. In principle, there could be other D-brane instantons having the desired intersection numbers, and such a brane might induce Majorana masses. However, such a situation does not happen, except in special cases. Though the number of zero modes is the same, the Majorana mass term may be canceled by the antisymmetric tensor or sign condition of equation (3.6). In more realistic models, other D-branes ignored in our analysis may intersect E-branes and spoil the zero-mode structure. Studying the effects of several E-branes is interesting work, but it is difficult to build a configuration with several E-branes inducing Majorana masses. Even if several configurations of an E-brane can induce nonzero Majorana masses, their effects are suppressed by the volumes of cycles wrapped by the E-branes, and one configuration would be dominant. To show it, we study the possibility of other E-branes in model 1-(I) in Appendix B.

[28] G. Altarelli and F. Feruglio, Discrete flavor symmetries and models of neutrino mixing, Rev. Mod. Phys. **82**, 2701 (2010).

[29] H. Ishimori, T. Kobayashi, H. Ohki, Y. Shimizu, H. Okada, and M. Tanimoto, Non-Abelian discrete symmetries in particle physics, Prog. Theor. Phys. Suppl. **183**, 1 (2010); Lect. Notes Phys. **858**, 87 (2012).

[30] S. F. King and C. Luhn, Neutrino mass and mixing with discrete symmetry, Rep. Prog. Phys. **76**, 056201 (2013).

[31] T. Kobayashi, H. P. Nilles, F. Ploger, S. Raby, and M. Ratz, Stringy origin of non-Abelian discrete flavor symmetries, Nucl. Phys. **B768**, 135 (2007).

[32] H. Abe, K. S. Choi, T. Kobayashi, and H. Ohki, Non-Abelian discrete flavor symmetries from magnetized/intersecting brane models, Nucl. Phys. **B820**, 317 (2009).

[33] M. Berasaluce-Gonzalez, P. G. Camara, F. Marchesano, D. Regalado, and A. M. Uranga, Non-Abelian discrete gauge symmetries in 4d string models, J. High Energy Phys. 09 (2012) 059.

[34] H. Abe, K. S. Choi, T. Kobayashi, and H. Ohki, Three generation magnetized orbifold models, Nucl. Phys. **B814**, 265 (2009).

[35] K. A. Olive *et al.* (Particle Data Group Collaboration), Review of particle physics, Chin. Phys. C **38**, 090001 (2014).

[36] D. V. Forero, M. Tortola, and J. W. F. Valle, Global status of neutrino oscillation parameters after Neutrino-2012, Phys. Rev. D **86**, 073012 (2012).